Exploring the Role of Sodium-Glucose Cotransporter as a New Target for Cancer Therapy

Ahmad M. Issa and Sanaa K. Bardaweel

Department of Pharmaceutical Sciences, School of Pharmacy, University of Jordan, Amman, Jordan

Corresponding author: Sanaa K. Bardaweel, Department of Pharmaceutical Sciences, School of Pharmacy, The University of Jordan, Queen Rania Street, Amman 11942, Jordan; Tel: 0096265355000 (ext. 23318); email: s.bardaweel@ju.edu.jo

Received, May 9, 2022; Revised, July 20, 2022; Accepted, July 20, 2022; Published, August 5, 2022

ABSTRACT – Purpose: To evaluate the effects of SGLT2 inhibitors on the proliferation, tumorigenesis, migration, colony formation, apoptosis, selected gene expression pattern, and combination with known chemotherapeutic drugs in different human cancer cell lines. **Methods:** The antiproliferative and combined effects of SGLT2 inhibitors were evaluated by MTT assay. Cell migration was assessed using wound-healing and colony formation assays. Apoptosis assay was conducted using annexin V-FITC/ propidium iodide staining. SGLT2 gene expression was determined using real-time PCR. **Results:** Canagliflozin, dapagliflozin, and ipragliflozin significantly inhibited the growth of different cancer cell lines in a dose and time-dependent manner. IC_{50} values after 48 hours of treatment with canagliflozin, ipragliflozin, and dapagliflozin ranged from 41.97 µM to 69.49 µM, 63.67 µM to 255.80 µM, and 167.7 µM to 435.70 µM in the examined cancer cell lines, respectively. The combined treatment of SGLT2 with doxorubicin and raloxifene separately resulted in a synergistic effect in Caco-2 and A-549 cell lines. On the other hand, the combination of SGLT2 inhibitors with cisplatin resulted in an antagonistic effect in A-549, Du-145, and Panc-1 cell lines. Canagliflozin and ipragliflozin inhibited cell migration and colony formation ability at IC_{50} and Sub-IC_{50} in the examined cancer cell lines. Canagliflozin and ipragliflozin significantly induced apoptosis at IC_{50} and Double-IC_{50} in the Du-145 cell line compared to the control. Real-time PCR showed that the treatment with 0.1 IC_{50} and 0.2 IC_{50} of both canagliflozin and ipragliflozin resulted in diminished RNA expression of SGLT2, VEGF, and Bcl-2 genes in the Du-145 cell line. **Conclusion:** SGLT2 inhibitors have antiproliferation, anti-tumorigenesis, and anti-migration effects and may induce apoptosis in cancer cells. In addition, treatment with SGLT2 inhibitors resulted in the downregulation of selected genes in the Du-145 cell line.

INTRODUCTION

Glucose, the key element for metabolic energy, is imported into cells by two classes of transporters: facilitative glucose transporters (GLUTs) and secondary active sodium-glucose cotransporters (SGLTs) (1). Increased demand and utilization for glucose uptake are demonstrated in cancer cells compared to normal cells. The overexpression of GLUTs, mainly GLUT1, in many cancer types has been reported in the literature (2-4). Recently, the functional activity of SGLT in different types of cells has been also reported (5, 6), yet poorly investigated in cancer.

Globally, cancer is a serious growing health problem with 19.3 million cases diagnosed in 2020 (7). There is evidence supporting the association between diabetes and cancer such that diabetic patients, predominantly with type 2 diabetes, are at greater risk of developing cancer (8). Increased level of circulating insulin is common in diabetic patients. Insulin resistance and reduced production of insulin growth factor binding protein (IGFBP) 1 and 2 lead to increasing the insulin receptor (IR), insulin growth factor 1 (IGF), and its receptor (9). IR, IGF-1, and its receptor are overexpressed in the cancer cell which may promote cell proliferation and protein synthesis and may protect cancer cells from apoptosis (8).

Many diabetic patients are obese, resulting from insulin resistance, which causes excess weight and obesity (10). Obesity contributes to tumor growth and metastasis by changing the function of adipose tissue leading to increased secretion of leptin, adiponectin, free fatty acid, proinflammatory cytokines, proangiogenic factor, and extracellular matrix constituents. Also, causing a hypoxic state due to the expansion of adipose tissue that leads to the infiltration of the macrophages, T cells, and natural killer (NK) cells. These cells secrete large amounts of proinflammatory cytokines that all play important roles in cancer development and

progression (11, 12). In addition, obesity increases the levels of gut metabolite deoxycholic acid by altering intestinal permeability and function causing DNA damage (10). Obesity can increase the estrogen level through a high conversion rate of androgenic precursor to estradiol by aromatization. DNA mutagenesis risk is increased with a higher concentration of circulating sex steroids and a lower concentration of sex hormone binding globulin (13).

The endoplasmic reticulum is responsible for the maturation of proinsulin to insulin. In diabetic patients, the production of insulin is increased because of insulin resistance with the increased level of glucose, and free fatty acid, leading to endoplasmic reticulum stress. Chronic endoplasmic reticulum stress promotes cancer cell survival and tumor growth (14). Lysosomes and proteasomes are the two major pathways of the degradation system for eukaryotic cells. Generally, the proteasome targets short-lived protein via the ubiquitin-proteasome system while, the lysosome targets long-lived protein and damaged intracellular organelles by autophagy. Autophagy is inhibited by hyperinsulinemia which enhances the tumor progression (14).

The hyperglycemic state is considered a suitable environment for the development and growth of cancer cells. Interestingly, to perform a high glycolysis rate, the expression of SGLT and GLUT in cancer cells is higher than in normal cells (15-17). In cancer, it has been found that the SGLT1 is overexpressed in the colon, pancreas, breast, and ovaries (6, 15, 18), while the SGLT2 is overexpressed in the lung, breast, pancreas, prostate, colon, and kidney (16).

Phlorizin, the first SGLT inhibitor, was introduced in 1853. It lowers the glucose concentration. However, phlorizin is easily hydrolyzed and poorly absorbed in the intestine. Extensive structural modifications have been made that resulted in the discovery of several SGLT inhibitors with different selectivity (19). Satogliflozin is a dual SGLT 1/2 inhibitor. Several other SGLT2 inhibitors have been identified including dapagliflozin, canagliflozin, empagliflozin, tofogliflozin, ipragliflozin, ertugliflozin, and luseogliflozin (20).

Dapagliflozin, ipragliflozin, and canagliflozin are considered selective inhibitors for SGLT2 (21). In the current study, the effect of different SGLT2 inhibitors on the viability, migration, and apoptosis of different cancer cell lines was investigated. In addition, the ability of SGLT2 inhibitors to modulate the antitumor effect of other anticancer drugs was also assessed as well as the underlying molecular mechanism driving the antiproliferative activity of SGLT2 inhibitors.

To our knowledge, this is the first study to evaluate the antiproliferative and antitumorigenic activity of different SGLT2 inhibitors on various cancer cell lines. Moreover, this is the first report to establish the relative expression of SGLT2, vascular endothelial growth factor (VEGF), and B-cell lymphoma 2 (Bcl-2) genes in a human prostate cancer cell line.

METHODOLOGY

Cell lines, culture conditions, and treatments preparation

Human lung (A-549), breast (MCF-7), colorectal (Caco-2), pancreatic (Panc-1), and prostate (Du-145) cancer cells were purchased from the American Type Culture Collection (ATCC, USA). A-549 and MCF-7 were cultured in Roswell Park Memorial Institute medium (RPMI) (Euro bio, French), Caco-2, Panc-1, and Du-145 were cultured in Dulbecco's Modified Eagle's Medium (DMEM) (Euro bio, French). Culture media were supplemented with 10% Fetal bovine serum (FBS) (Capricorn Scientific GmbH, Germany), 100 U/mL penicillin (Euro Clone, Italy), 0.1 mg/mL streptomycin (Euro Clone, Italy), and 2 mM L-glutamine (Euro Clone, Italy). Cells were maintained 75 cm^2 flask and incubated at 5% CO_2, and 95% humidified air at 37ºC.

Canagliflozin hemihydrate and ipragliflozin were purchased from BLD pharma, China. Doxorubicin hydrochloride 2 mg/mL was purchased from Ebewe Unterach, Austria. While raloxifene, cisplatin, and dapagliflozin propanediol monohydrate were purchased from Sigma-Aldrich, USA. Canagliflozin hemihydrate ($C_{48}H_{52}F_2O_{11}S_2$) MM= 907.05 g/mol, ipragliflozin ($C_{21}H_{21}FO_5S$) MM= 404.45 g/mol, dapagliflozin propanediol monohydrate ($C_{24}H_{35}ClO_9$) MM= 502.98 g/mol, and raloxifene ($C_{28}H_{27}NO_4S$) MM=473.6 g/mol, were dissolved in DMSO at an appropriate concentration (50000 µM for canagliflozin, ipragliflozin, and dapagliflozin, while raloxifene at a concentration of 30000 µM). The final concentration of Dimethyl Sulfoxide (DMSO) (Santa Cruz Biotechnology, USA) was ensured not to exceed 1% in the well. Cisplatin ($Pt(NH_3)2Cl_2$) MM= 300.05 g/mol was dissolved in 0.9% sodium chloride solution at a final concentration of 0.6 mg/mL.

Doxorubicin, C27H29NO11·HCl [molar mass (MM), 580.0 g/mol] was supplied as a concentrated

solution for injection. Further dilution was carried out using the appropriate medium as needed to reach the target concentration immediately before use.

Cell viability

For assessing cell proliferation, the 3-(4,5-dimethylthiazol-2-yl) -2,5-diphenyltetrazolium-bromide (MTT) was used (22). All cells were seeded in 96 well plates at a concentration of 8000 cells per well except Caco-2 at a concentration of 10000 cells per well. A-549 and MCF-7 were seeded in RPMI medium while other cells were seeded in DMEM medium. After 24 h of incubation at 37ºC in a humidified incubator set with 95% humidity, and 5% CO_2, the medium was discarded, and cells were treated with a medium containing drug at different concentrations. In addition, negative control wells containing only medium and DMSO were prepared under the same conditions.

After treatment for 24 h, 48 h, and 72 h, 10 µl of MTT dye at a working concentration of 5 mg/mL was added to each well and incubated for 3 h at 37ºC in a humidified incubator set at 95% humidity, and 5% CO_2. Afterward, the medium was aspirated using a 1 mL insulin syringe then 100 µl DMSO was added to each well, and plates were kept on an orbital shaker at 150 PPM for 15 minutes in a dark room. Optical density was measured at 570 nm using a microplate reader.

All experiments were run in duplicate wells and repeated three times (n=6). IC_{50} was calculated using GraphPad Prism 8 software, (GraphPad Software, San Diego, USA).

Drug combination

All cells were seeded in 96 well plates at a concentration of 8000 cells per well except Caco-2 at a concentration of 10000 cells. A-549 and MCF-7 were seeded in RPMI medium while other cells were seeded in DMEM medium. To evaluate the combined effect of SGLT2 inhibitors with cisplatin, doxorubicin, and raloxifene, various concentrations of the examined combination at ratios 1:5, 1:10 were applied on cells for 48 h. Then MTT assay was performed, and optical density was measured at 570 nm. The combination index (CI) was then calculated using CompuSyn software (Combosyn Inc., Paramus, NJ, USA).

Colony formation in soft agar

A colony formation assay was used to evaluate the ability of the cancer cells to form a colony via anchorage-independent- growth (23). To perform the soft agar colony formation assay, a base layer of 0.6% (w/v) noble agar was prepared in a 6-well plate by adding autoclaved 1% agar solution to sterile filtered and warm 2X full DMEM medium in a 1:1 ratio and allowed to settle and solidify at room temperature. Each soft-agar layer required 2 mL (1 mL media + 1 mL agar) to cover the 6-well surface properly. For the upper 0.3% noble agar layer, we counted 50,000 A-549 cells which all were pre-treated for 48 h with either sub- IC_{50} or IC_{50} concentrations of SGLT2. The treated cells were then mixed with 0.6% (w/v) noble agar in a 1:1 ratio and poured on top of the base layer, then allowed to settle and solidify for 30 mins at room temperature. Plates were incubated for 2 weeks in a humidified controlled temperature incubator set at 37ºC, 95% humidity, and 5% CO_2 and fortified gently with 100-200 µl of DMEM full media twice weekly to prevent dissection of agar. Images were captured within 14 days at several magnifications using the EVOS XL Core imaging system (Invitrogen, USA).

Migration

The wound healing assay was used to assess cell movements in two dimensions (24). A-549, Du-145, and Panc-1cells were seeded in inserts (Ibidi, Germany) at a concentration of 30000 per insert in a 70 µl medium and incubated for 24 h. Afterward, inserts were removed, and cells were incubated with 10 µg/mL of mitomycin C for 2 h to stop cell proliferation. The medium was removed, and cells were washed three times then cells were treated with IC_{50} or sub-IC_{50} concentrations of SGLT2; canagliflozin, or ipragliflozin. Images were captured at 0 and 24 hours using the EVOS XL Core imaging system at 10x magnification. Wound width was measured using Image J Software Ver.1.53e.

Annexin V-FITC /Propidium Iodide apoptosis

The Du-145 cells were plated in 6-well plates at a concentration of 300000 cells per well in a 3 mL medium and allowed to attach overnight. The cells were then treated with IC_{50} or double IC_{50} concentration for SGLT2 while cisplatin was used as a positive control. Negative control wells containing only medium were included in the experiment. After 48h incubation, floating cells were collected, and the attached cells were resuspended in 500 µl cold PBS and centrifuged. The pellets were resuspended in 1X binding buffer (200 µL) then cells were stained with 5µl Annexin V-FITC and incubated for 5 min at room temperature, Propidium iodide (PI) (50 µg/mL) was then added to each tube and analyzed

immediately. The analysis was performed on a BD FACSCanto II flow cytometer (BD Biosciences, USA) using BD FACSDiva software (BD Biosciences, USA).

Real-time polymerase chain reaction (qPCR)

The Du-145 cells were seeded at a density of 300000 cells/ well in a 6 well-plate and incubated for 24 h. Du-145 cells were treated with 0.1 IC_{50} and 0.2 IC_{50} of SGLT2 inhibitors; canagliflozin and ipragliflozin for 48 h. Afterward, the total RNAs of cells were purified as previously prescribed [25]. qPCR was performed using an SYBR Green Real-time PCR Master Mix and the Applied Biosystems 7500 real-time PCR detection system. The primer sequences used are shown in Table S1**.**

Thermal cycling conditions for SGLT2 were as the following: cDNA was initially denatured at 95 ºC for 15 min, 40 cycles at 95 ºC for 15 sec, followed by 53 ºC for 30 sec, and 72 ºC for 60 sec. For Bcl-2 and VEGF, initial denaturation at 95 ºC for 15 min, followed by 45 cycles of 95 ºC for 10 sec, 59 ºC for 30 sec, and 72 ºC for 30 sec. For glyceraldehyde 3-phosphate dehydrogenase (GAPDH), initial denaturation at 95 ºC for 15 min, followed by 45 cycles for 95 ºC for 15 sec, 58 ºC for 30 sec, and 72 ºC for 30 sec. Expression changes were normalized to the GAPDH gene using the ΔΔCt method.

Statistical Analysis

Statistics

Data analysis was performed using GraphPad Prism software (GraphPad Prism version 8.0.2 for Windows, GraphPad Software, San Diego, California USA) and a statistical package for the social sciences software (IBM Corp. Released 2016. IBM SPSS Statistics for Windows, Version 24.0. Armonk, NY: IBM Corp.). The differences between treatment groups were determined by two-way analysis of variance ANOVA where feasible followed by an appropriate post hoc test. Data are expressed as mean± SD and $p < 0.05$ is considered a statistically significant difference.

The non-linear regression analysis was used to calculate IC_{50} values. The combination index (CI) was calculated using CompuSyn software (Combosyn Inc., Paramus, NJ, USA), which is based on Chou-Talalay's Combination Index Theorem. The wound area was measured using ImageJ software Version 1.53e. Colony size and numbers were measured according to color threshold using ImageJ software.

RESULTS

Effect of SGLT2 inhibitors on cell viability

To evaluate the effect of SGLT2 inhibitors treatment (canagliflozin, ipragliflozin, and dapagliflozin) on the viability of different cancer cell lines, an MTT assay was carried out using A-549, Caco-2, MCF-7, Du-145, and Panc-1 cell lines. Various concentrations of SGLT2 inhibitors were tested for 24, 48, and 72 h (1-500 µM of canagliflozin, 1-500 µM of ipragliflozin, 1-1000 µM of dapagliflozin). Additionally, to determine the 50% inhibitory concentration of selected standard chemotherapy agents, the MTT assay was carried out on different cell lines. Several concentrations were tested for 24, 48, and 72 h (1-200 µM of cisplatin, 1-200 µM of doxorubicin, and 1-100 µM of raloxifene).

Table 1 Depicts the 50% inhibitory concentration (IC_{50}) for the canagliflozin, ipragliflozin, dapagliflozin, cisplatin, doxorubicin, and raloxifene against A-549, Caco-2, MCF-7, Du-145, and Panc-1 cells while Figure 1**,** shows the statistical significance of the differences.

Effect of combined treatment of SGLT2 inhibitors and chemotherapeutic

To determine the effect of combined SGLT2 inhibitors with different chemotherapeutics agents, canagliflozin and ipragliflozin were combined with cisplatin, doxorubicin or raloxifene at ratios of 1:5, 1:10 (chemotherapeutics agents: SGLT2 inhibitors) and incubated for 48 h (Table 2S). The combination of doxorubicin with ipragliflozin at a ratio of 1:10 significantly reduced IC_{50} of ipragliflozin for MCF-7 inhibition by 7.8 fold. In general, the combination of SGLT2 inhibitors with cisplatin in A-549, Du-145, and Panc-1 cell lines resulted in an antagonistic effect with a combination index (CI) >1, while the combination of SGLT2 inhibitors with either doxorubicin or raloxifene resulted in a synergistic effect with a combination index <1 in the same cell lines (Table 3S.)

Effect of SGLT2 inhibitors on the migration of cancer cells

To assess the effect of SGLT2 inhibitors on the 2D migration of different cell lines a wound healing assay was carried out using both IC_{50} and sub-IC_{50} concentrations of either canagliflozin or ipragliflozin on A-549, Du-145, and Panc-1 cell lines. After 24 h, complete or almost complete closure of the artificial wound in the untreated samples was observed. SGLT2 inhibitor treatment led to the inhibition of cell migration compared to untreated cells.

Table 1. 50% Inhibitory concentrations (IC_{50})

	Time, h	Cell line				
		A-549	Caco-2	MCF-7	Du-145	Panc-1
Canagliflozin IC_{50} (µM)						
	24	**99.6**	**144.5**	**69.9**	**73.6**	**64.8**
	48	**69.4**	**48.4**	**41.9**	**43.7**	**45.8**
	72	**64.1**	**27.8**	**35.7**	**30.8**	**26.9**
Ipragliflozin IC_{50} (µM)						
	24	**457.9**	**415.8**	**112.6**	**439.0**	**388.5**
	48	**204.4**	**168.5**	**63.6**	**158.1**	**255.8**
	72	**170.5**	**150.6**	**56.1**	**106.7**	**112.7**
Dapagliflozin IC_{50} (µM)						
	24	**441.3**	**259.2**	**404.6**	**883.4**	**609.2**
	48	**287.5**	**167.8**	**243.4**	**290.1**	**435.7**
	72	**286.9**	**115.7**	**143.1**	**243.1**	**160.3**
Cisplatin IC_{50} (µM)						
	24	**69.6**	**NA**	**NA**	**176.2**	**117.0**
	48	**44.5**	**NA**	**NA**	**5.8**	**33.5**
	72	**34.2**	**NA**	**NA**	**3.7**	**23.7**
Doxorubicin IC_{50} (µM)						
	24	**NA**	**52.3**	**42.5**	**NA**	**NA**
	48	**NA**	**8.9**	**9.0**	**NA**	**NA**
	72	**NA**	**4.0**	**5.6**	**NA**	**NA**
Raloxifene IC_{50} (µM)						
	24	**74.3**	**NA**	**48.1**	**NA**	**NA**
	48	**40.8**	**NA**	**30.5**	**NA**	**NA**
	72	**30.1**	**NA**	**22.0**	**NA**	**NA**

For statistical significance of differences see Figure 1. Determinations were done in duplicate at least three times (n=6); The standard deviation of none of the IC_{50} values exceed 5%. NA: not available.

Treatment of cells with Canagliflozin resulted in approximately 2% of wound closure (98% inhibition of wound closure) at both IC_{50} and sub-IC_{50} concentrations for the Panc-1 cell line (Figure 2).

Effect of SGLT2 inhibitors on apoptosis of prostate cancer cell

To examine whether SGLT2 inhibitors affected prostate cancer cell viability via induction of apoptosis or necrosis, annexin V-FITC /PI double staining was performed. As shown in Figure 3, treatment of Du-145 cells with IC_{50} or double IC_{50} concentration of either canagliflozin and ipragliflozin separately resulted in a significant increase in early and late apoptosis compared to the respective untreated control groups. As shown in Figure 3, canagliflozin and ipragliflozin at double IC_{50} had significantly induced apoptosis in the Du-145 cell line (78.7% and 30.8%) compared to control cells.

Effect of SGLT2 inhibitors on colony formation of cancer cells

To investigate the effect of SGLT2 inhibitors treatment on the colony formation capability of cancer cells, A-549 cancer cells were treated with sub-IC_{50} and IC_{50} concentrations of canagliflozin and ipragliflozin for 48 h, separately. Afterward, cells were grown on soft noble agar. The results showed that SGLT2 inhibitors treatment inhibited the formation of colonies by reducing the number and the size of formed colonies of the A-549 cell line relative to the untreated control groups. Representative images were taken on day 14 and are shown in Figure 4**.** The mean colony size and number of colonies formed in the treated cells relative to the control group is shown in Figure 5**.**

Effect of SGLT2 inhibitors on multiple gene expression of prostate cancer cell

To determine the treatment effect of SGLT2 inhibitors treatment on Du-145 cells' expression of SGLT2, Bcl-2, and VEGF, the expression level of each gene was detected by qPCR in Du-145 cells after treatment with either 0.1 IC_{50} or 0.2 IC_{50} concentration of canagliflozin and/or ipragliflozin for 48 h then it was compared to the expression level in the baseline untreated Du-145 cancer cells. Compared to control groups, the treatment with either canagliflozin and/or ipragliflozin over time resulted in decreasing the transcription or RNA expression of SGLT2, Bcl-2, and VEGF as shown in Figure 6.

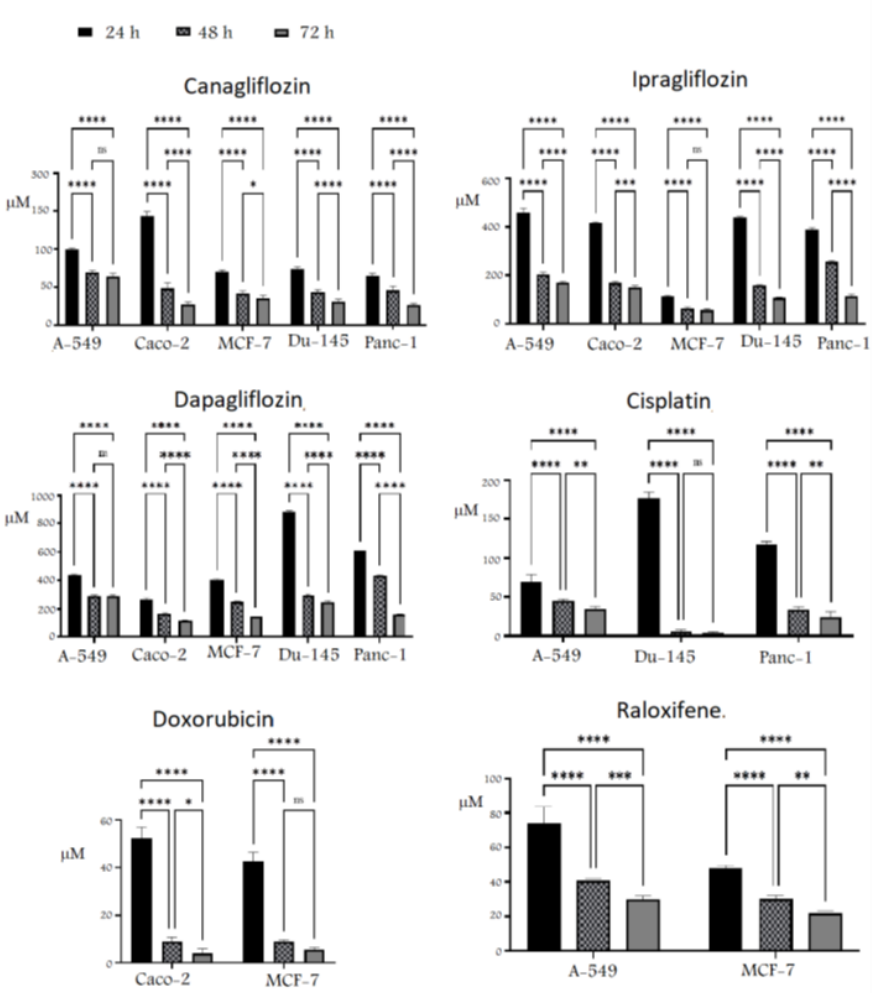

Figure 1. Time-dependent inhibition of A-549, Caco-2, MCF-7, Du-145, and Panc-1 cells at 24 h, 48 h, and 72 h treatment duration by various drugs at IC_{50}**.** The data shown represent IC_{50} ± SD. IC_{50} was calculated using Prism software. Cells were cultured and allowed to attach overnight. On the next day of culture, cells were treated with different concentrations of canagliflozin, dapagliflozin, ipragliflozin, cisplatin, doxorubicin, and raloxifene to determine the IC_{50}. Afterward, the IC_{50} was calculated to assess the inhibitory effect at three different incubation times. Each experiment was performed in duplicate and repeated at least three times independently. P-value <0.05 indicates statistical significance, while asterisk: ns (not-significant) $P > 0.05$; *$P \leq 0.05$; ** $P \leq 0.01$; *** $P \leq 0.001$; **** $P \leq 0.0001$ (according to GraphPad prism 8). μM: micromolar.

DISCUSSION

Glycolysis is a metabolic pathway that produces energy in cancer cells even in the absence of oxygen (26). The increased uptake of glucose and its metabolism mediated by SGLT2 in a cancer cell is higher than in normal cell (27). Many studies have shown that SGLT2 is overexpressed in several cancer types including lung, breast, and pancreatic (28-30). According to the results of the current study, canagliflozin, dapagliflozin, and ipragliflozin significantly inhibited cell proliferation of the examined cell lines of A-549, Caco-2, MCF-7, Du-145, and Panc-1 in time and concentration-dependent manner compared to the respective untreated control cells.

The variability in the activity of SGLT2 inhibitors reflected as the difference in the selectivity of these SGLT2 inhibitors for SGLT2. Several studies had demonstrated that the selectivity of dapagliflozin for SGLT2 over SGLT1 is higher than canagliflozin and ipragliflozin (31). Another factor that may have contributed to the difference in the activity of SGLT2 inhibitors in the examined cell lines relates to their different molecular subtypes and the expression pattern of SGLT2.

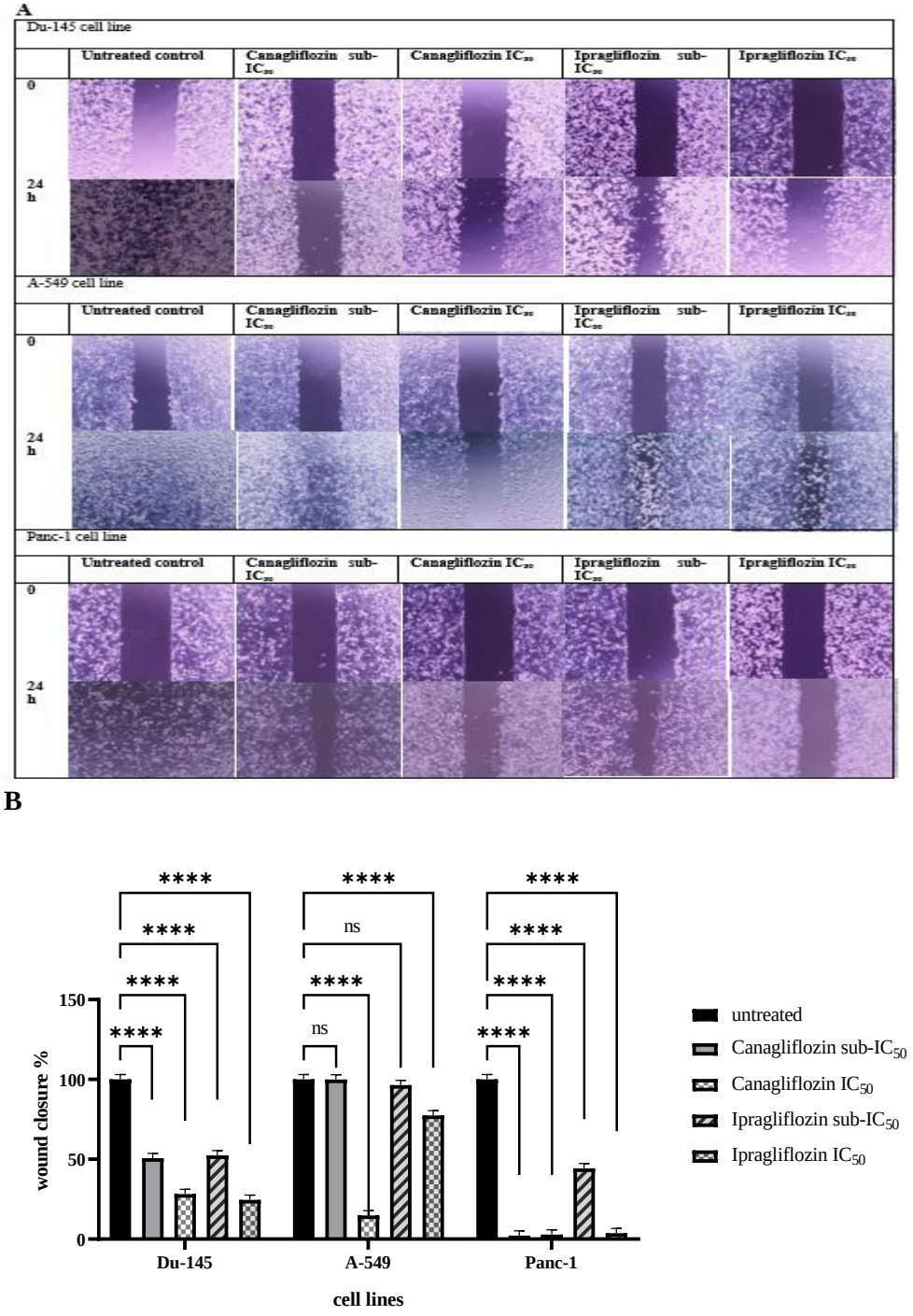

Figure 2. Effect of SGLT2 inhibitors, Canagliflozin and Ipragliflozin, on cancer cell migration. A. Images of the wounds at time zero and 24 h post-treatment. B. Quantitative analysis of the percentage wound closure relative to wound distance at time 0. Cancer cells were seeded in inserts and incubated overnight for attachment and confluency. Afterward, inserts were removed and cells were treated with mitomycin C for 2 h to stop cell proliferation. Then cancer cells were treated with canagliflozin and ipragliflozin separately at IC_{50} and sub-IC_{50} concentrations for 24h. Each experiment was performed in duplicate in three independent trials (n=6). P-value < 0.05 express significantly different from respective untreated condition; while asterisk: ns (not-significant) $P > 0.05$; * $P \leq 0.05$; ** $P \leq 0.01$; *** $P \leq 0.001$; **** $P \leq 0.0001$ (according to GraphPad prism 8).

Cisplatin is considered the cornerstone chemotherapeutic treatment in numerous human cancers including lung, brain, pancreas, head and neck, ovarian, and prostate cancer (32). It induces cytotoxic properties through crosslinks with the purine bases on the DNA causing DNA damage (32). This study demonstrated that the combination of either canagliflozin or ipragliflozin with cisplatin decreased the therapeutic effect of both drugs and contributed to antagonistic effect in A-549, Du-145,

A

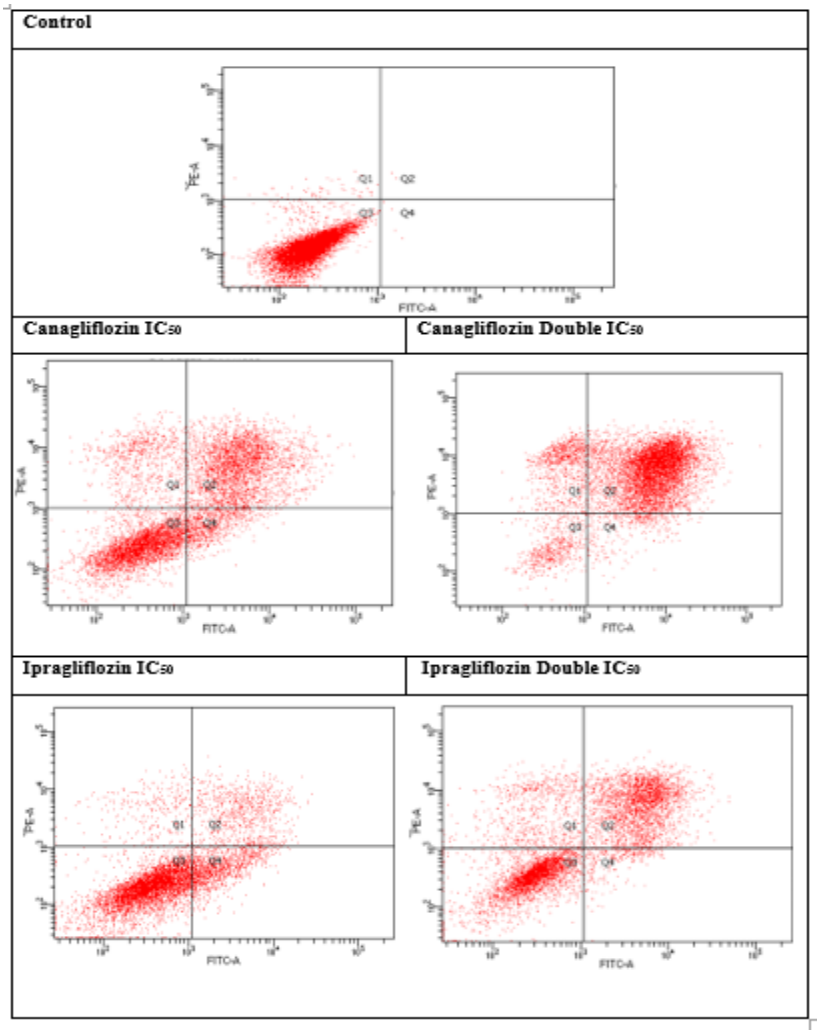

B

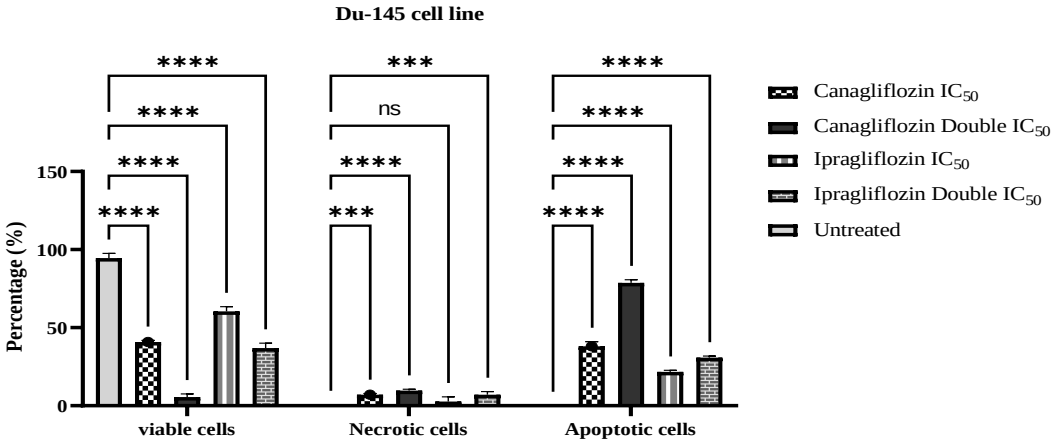

Figure 3. A. Dot plot for annexin V-FITC/ PI staining expressing the effect of SGLT2 inhibitors. Where Q3 shows healthy viable cells, Q1 necrotic cells, Q2 late apoptotic, and Q4 early apoptotic. B. Percentages of healthy, apoptotic, and necrotic cells expressed effect SGLT2 inhibitors. The experiment was performed in duplicate and repeated in two independent trials (n=4). P-value < 0.05 express significantly different from respective untreated cells' status; while asterisk: ns (not-significant) P > 0.05; * P ≤ 0.05; ** P ≤ 0.01; *** P ≤ 0.001; **** P ≤ 0.0001 (according to GraphPad prism 8). The standard deviation of values did not exceed 5%.

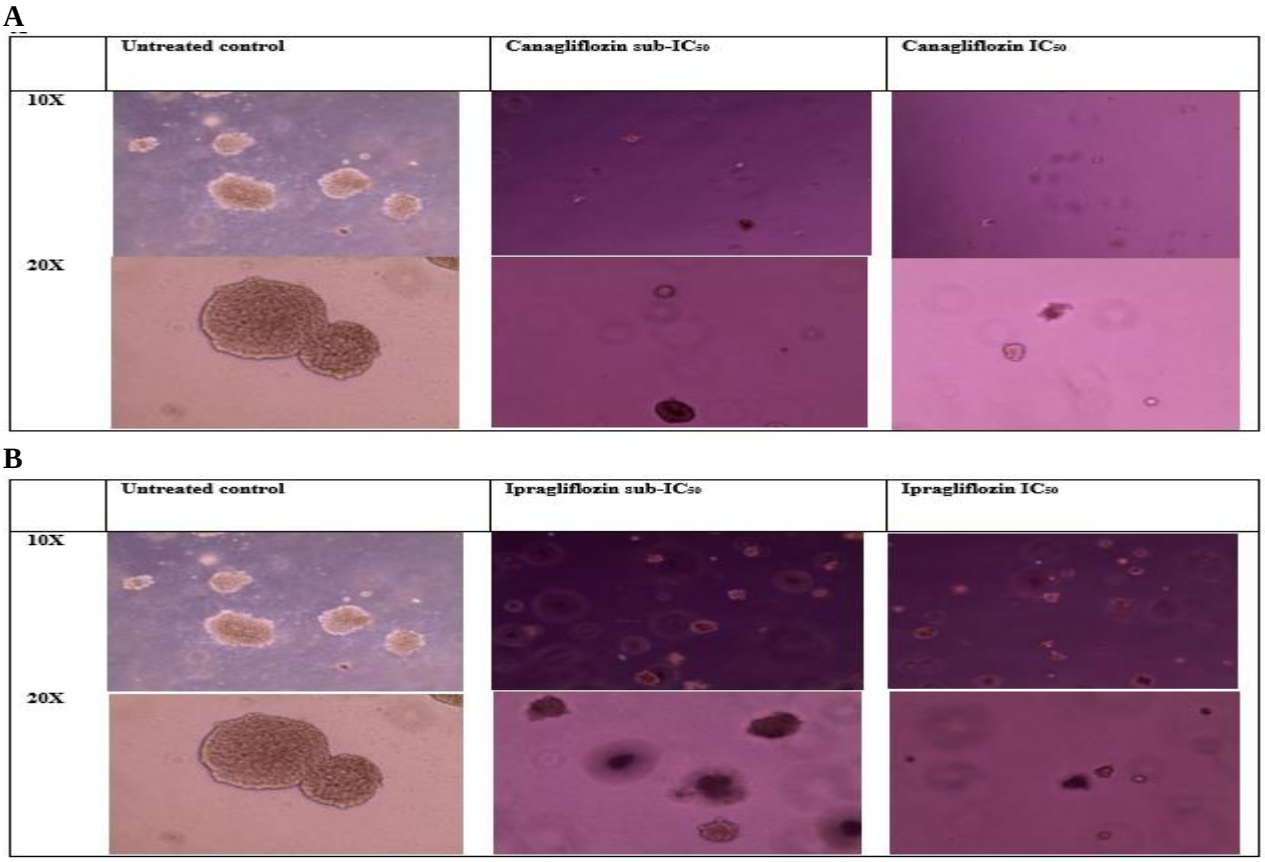

Figure 4. Images show colonies of different cancer cells at different magnifications (10X and 20X). A. Effect of canagliflozin on A-549 lung cancer cell line using colony formation assay. B. Effect of ipragliflozin on A-549 lung cancer cell line using colony formation assay. Cells were routinely seeded and treated with canagliflozin and ipragliflozin sub- IC_{50} and IC_{50} concentrations for 48 h separately, after that cell were counted and calculations were carried out to withdraw 50,000 of A-549 which were incorporated in the upper soft-agar layer and incubated for 14 days.

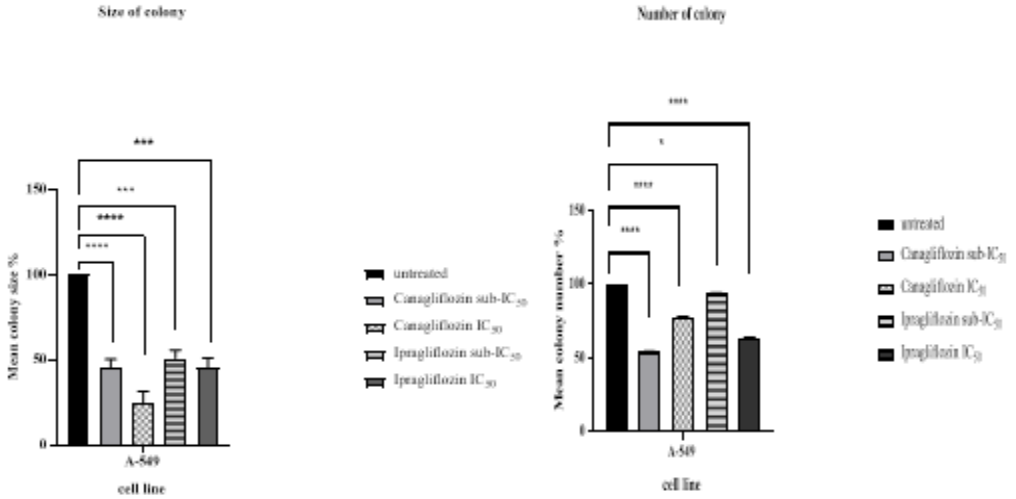

Figure 5. Effect of SGLT2 inhibitors on A-549 cancer cell line using colony formation assay. P-value < 0.05 express significantly different from respective untreated cells' status; while asterisk: ns (not-significant) $P > 0.05$; * $P \leq 0.05$; ** $P \leq 0.01$; *** $P \leq 0.001$; **** $P \leq 0.0001$ (according to GraphPad prism 8). Standard deviation of values did not exceed 5%. IC_{50}: The 50% inhibitory concentration.

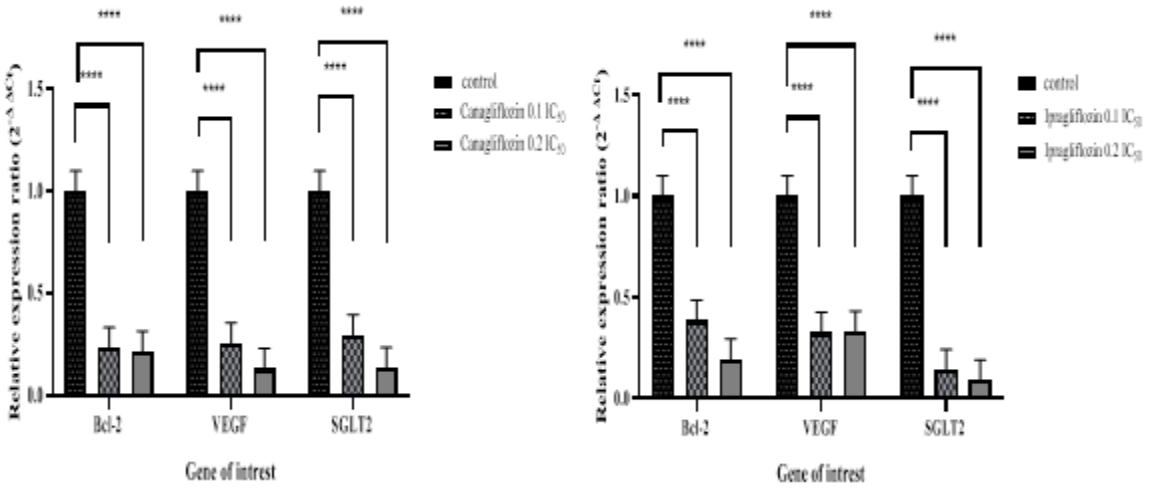

Figure 6. Effect of canagliflozin and ipragliflozin, on multiple RNA expression of specific genes in Du-145 prostate cancer cell line. SGLT2: the gene for Sodium-glucose cotransporter; Bcl-2: the gene for B-cell lymphoma 2; VEGF: the gene for Vascular endothelial growth factor. Fold difference was expressed as mean ± SD and was measured using the ΔΔCt method. All experiments were run in duplicates and with three independent experiments. P-value < 0.05 express significantly different from respective normal cells' status; while asterisk: ns (not-significant) P >0.05; * P ≤ 0.05; ** P ≤ 0.01; *** P ≤ 0.001; **** P ≤ 0.0001 (according to GraphPad prism 8).

and Panc-1. Studies have reported that treatment with canagliflozin, suppressed cisplatin-induced p53 phosphorylation and mitogen-activated protein kinase (MAPK) signaling pathway activation, DNA repair, angiogenesis, and autophagy (33, 34) resulting in an antagonistic effect. Canagliflozin increased Akt activation to prevent cisplatin-induced cellular apoptosis by activating the phosphatidylinositol 3-kinase pathway (34).

Doxorubicin inhibits topoisomerase II and generates free radicals causing cell membrane damage (35). The present study reveals that there is a significant increase in the therapeutic effect and synergistic improvement of both treatments in Caco-2 and MCF-7 when combined with canagliflozin or ipragliflozin for 48 h. Evidence suggests that the combined treatment of SGLT2 inhibitors and doxorubicin may increase the intracellular doxorubicin level by reducing the P-glycoprotein (P-gp) activity (36). P-gp efflux is an ATP-dependent pump and combining canagliflozin with doxorubicin may reduce the intracellular ATP by inhibiting glycolysis (36).

Raloxifene is a second generation of selective estrogen receptor modulators (SERMs) (37). Al-Sous *et al*. have characterized the estrogen receptor expression in lung cancer cells and demonstrated the potential benefits of SERMs in the treatment of lung cancer (38). Our study shows that in A-549, combining canagliflozin or ipragliflozin with raloxifene decreased cell survival and resulted in a synergistic effect compared to the mono-therapeutic regime of each drug.

Cell migration is a complex and heterogeneous process by which cells move from one location to another (39). Cells may migrate as a single cell mediated by cytoskeletal activity without interaction with the neighboring cells (40). The cytoskeleton is a complex, dynamic network and it is composed of three main components, microfilaments, intermediate filaments, and microtubules. Besides its primary function to preserve the cells' shape and prevent cell deformation, the cytoskeleton can contract to allow the cell to migrate (39). Collective cell migration is characterized as a cohesive cell group that retains cellular junctions and coordinates cytoskeletal activity between neighboring cells as well as with the surrounding tissues (40).

Evidence suggests that cancer cell migration is regulated by different signaling pathways including, vascular endothelial growth factor (VEGF) signaling in colorectal cancer, focal adhesion kinase (FAK) signaling in a variety of cancer, such as breast, lung, prostate, colon, and ovary (41, 42). Cancer cell migration was inhibited through inhibition of both epidermal growth factor receptor (EGFR) and c-erbB2 protein has been found in many cancers such as bladder cancer, colorectal cancer, lung cancer, and breast cancer (43).

This study reveals the ability of SGLT2 inhibitors, canagliflozin, and ipragliflozin to inhibit A-549, Du-145, and Panc-1 cancer cells' migration in a concentration-dependent manner. Human tumor cells interact with each other to grow independently and form colonies in an anchorage-independent manner. Colony formation assay is commonly used to study the ability of cancer cells to colonize (44). Our results reveal the role of SGLT2 inhibitors to inhibit the anchorage-independent growth in lung cancer cell lines. Canagliflozin and ipragliflozin, at IC_{50} and Sub-IC_{50} concentrations, reduced colonies' number and size in A-549 lung cancer cell lines.

Apoptosis is described as an active, programmed/regulated process of independent cellular death that avoids eliciting inflammation, while necrosis is the passive, accidental cell death resulting from external stress factors with the uncontrolled release of inflammatory cellular contents (45).

This study has demonstrated that treatment of Du-145, prostate cancer cell line, with canagliflozin or ipragliflozin, had significantly induced apoptosis in a concentration-dependent manner when compared to the respective untreated control cells. The apoptotic effect of canagliflozin was previously observed in A-549 (46).

Real-time PCR is the technique to quantify gene expression throughout RNA isolation and cDNA synthesis (47). This study revealed that SGLT2 is overexpressed in Du-145 prostate cancer cell lines. Moreover, VEGF gene expression was significantly increased over time, which might be related to the hypoxic stressful environment of the cells and their ability to thrive to enhance angiogenesis (48). On the other hand, the expression of the Bcl-2 gene in cancer cells, a hallmark of cellular apoptosis regulation that is commonly related to cancer pathophysiology and resistance to conventional chemotherapy, has been shown to increase in many cancer cells (49). Interestingly, canagliflozin and ipragliflozin significantly decreased the gene expression of VEGF and Bcl-2.

CONCLUSION

In conclusion, this *in vitro* study demonstrated the potential clinical benefits of SGLT2 inhibitors in different cancer cell lines by showing that the canagliflozin, ipragliflozin, and dapagliflozin had significantly inhibited the growth of the A-549, MCF7, Caco-2, Du-145, and Panc-1 cell lines in a dose and time dependent manner. In addition, the combination of canagliflozin and ipragliflozin separately with cisplatin resulted in an antagonistic effect but the combination of canagliflozin and ipragliflozin separately with either doxorubicin or raloxifene resulted in a synergistic effect. This antiproliferative effect of canagliflozin and ipragliflozin was mediated through the induction of apoptosis in the Du-145 cell line. Moreover, canagliflozin and ipragliflozin inhibited cell migration and colony formation in the A-549 cell line. This study has also shown that Du-145 cell lines are positive for SGLT2 and SGLT2 inhibitors treatments resulting in significant downregulation of SGLT2, VEGF, and Bcl-2 gene expression compared to untreated cells.

CONFLICT OF INTEREST. The author declares there is no conflict of interest

FINANCIAL DISCLOSURE. The Deanship of Scientific Research at the University of Jordan, grant numbers 2349 and 2353 funded this research

AUTHORS' CONTRIBUTION.
Conceptualization, S.B.; methodology, A.I.; validation, S.B.; formal analysis, A.I.; investigation A.I..; resources, S.B.; writing—original draft preparation, S.B., A.I.; writing—review and editing, S.B.; supervision, S.B.; project administration, S.B.; funding acquisition, S.B. All authors have read and agreed to the published version of the manuscript.

REFERENCES

1. Ferrannini E. Sodium-glucose co-transporters and their inhibition: clinical physiology. Cell Metab, 2017. 26(1): p. 27-38. DOI: 10.1016/j.cmet.2017;04.011.
2. Sharen G, Peng Y, Cheng H, Liu Y, Shi Y, Zhoa J. Prognostic value of GLUT-1 expression in pancreatic cancer: results from 538 patients. Oncotarget, 2017; 8(12): p. 19760. DOI: 10.18632/oncotarget.15035.
3. Pezzuto A, D'Ascanio M, Ricci A, Paglianne A, Carico E. Expression and role of p16 and GLUT1 in malignant diseases and lung cancer: A review. Thorac cancer, 2020; 11(11): p. 3060-3070. DOI: 10.1111/1759-7714.13651.
4. Meziou S, Ringuette C, Hovington H, Lefebure V, Lavallée É, Bergeron M, et al. GLUT1 expression in high-risk prostate cancer: correlation with 18F-FDG-PET/CT and clinical outcome. Prostate Cancer and

Prostatic Dis, 2020; 23(3): p. 441-448. DOI: 10.1038/s41391-020-0202-x.
5. Szablewski L. Expression of glucose transporters in cancers. Biochim Biophys Acta Rev Cancer, 2013; 1835(2): p. 164-169. DOI: 10.1016/j.bbcan.2012.12.004
6. Perez M, Praena-Fernandez J, Felipe-Abrio B, Lopez-Garcia M, Lucena-Cacace A, GarciaA, et al. MAP17 and SGLT1 protein expression levels as prognostic markers for cervical tumor patient survival. PloS One, 2013; 8(2): p. e56169.
7. Sung H, Ferlay J, Siegel R, Laversanne M, Soerjomataram I, Jemal A, et al. Global cancer statistics 2020: GLOBOCAN estimates of incidence and mortality worldwide for 36 cancers in 185 countries. CA Cancer J Clin, 2021; 71(3): p. 209-249. DOI: 10.3322/caac.21660.
8. Garg S, Maurer H, Reed K, Selagamsetty R. Diabetes and cancer: two diseases with obesity as a common risk factor. Diabetes Obes Meta, 2014; 16(2): p. 97-110. DOI: 10.1111/dom.12124.
9. Pollak M. Insulin and insulin-like growth factor signalling in neoplasia. Nat Rev Cancer, 2008; 8(12): p. 915-928. DOI: 10.1038/nrc2536.
10. Avgerinos K, Spyrau N, Manzoros C, Dalamaga M. Obesity and cancer risk: Emerging biological mechanisms and perspectives. Metabolism, 2019; 92: p. 121-135. DOI: 10.1016/j.metabol.2018.11.001.
11. Abdel-Rahman O. Validation of the prognostic value of new sub-stages within the AJCC 8th edition of non-small cell lung cancer. Clin Transl Oncol, 2017; 19(11): p. 1414-1420. DOI: 10.1007/s12094-017-1673-7.
12. Basen-Engquist K, Chang M. Obesity and cancer risk: recent review and evidence. Curr oncol rep, 2011; 13(1): p. 71-76. DOI: 10.1007/s11912-010-0139-7.
13. Roberts D, Dive C, Renehan A. Biological mechanisms linking obesity and cancer risk: new perspectives. Annu Rev Med, 2010; 61: p. 301-316. DOI: 10.1146/annurev.med.080708.082713.
14. Hua F, Yu J, Hu Z. Diabetes and cancer, common threads and missing links. Cancer lett, 2016; 374(1): p. 54-61. DOI: 10.1016/j.canlet.2016.02.006.
15. Guo G, Cai Y, Zhang B, Xu R, Qiu H, Xia L, et al. Overexpression of SGLT1 and EGFR in colorectal cancer showing a correlation with the prognosis. Med Oncol, 2011; 28(1): p. 197-203. DOI: 10.1007/s12032-010-9696-8.
16. Wright E. SGLT2 and cancer. Pflugers Arch, 2020; p. 1-8. DOI: 10.1007/s00424-020-02448-4.
17. Benedetti R, Benincasa G, Glass K, Chianese U, Vietri M, Congi R, Altucci L, Napoli, et al. Effects of novel SGLT2 inhibitors on cancer incidence in hyperglycemic patients. Pharmacol Res, 2021: p. 106039. DOI: 10.1016/j.phrs.2021.106039
18. Casneuf V, Fonteyne P, Damme N, Demetter P, Pauwels P, hemptinne B, et al. Expression of SGLT1, Bcl-2 and p53 in primary pancreatic cancer related to survival. Cancer Invest, 2008; 26(8): p. 852-859. DOI: 10.3892/ol.2017.7218.
19. Jabbour S, Goldstein B. Sodium glucose co-transporter 2 inhibitors: blocking renal tubular reabsorption of glucose to improve glycaemic control in patients with diabetes. Int J Clin Pract, 2008; 62(8): p. 1279-1284. DOI: 10.1111/j.1742-1241.2008.01829.x.
20. Brown E, Rajeev S, Cuthbertson D, Wilding J. A review of the mechanism of action, metabolic profile and haemodynamic effects of sodium-glucose co-transporter-2 inhibitors. Diabetes, Obe Metab, 2019; 21: p. 9-18. DOI: 10.1111/dom.13650.
21. Cai W, Jiang L, Xie Y, Liu W, Zhao G. Design of SGLT2 inhibitors for the treatment of type 2 diabetes: a history driven by biology to chemistry. Med Chem, 2015; 11(4): p. 317-328. DOI: 10.2174/1573406411666150105105529.
22. Bardaweel S,Tawaha K, Hudaib M. Antioxidant, antimicrobial and antiproliferative activities of Anthemis palestina essential oil. BMC Complement Altern Med, 2014; 14(1): p. 1-8. DOI: 10.1186/1472-6882-14-297.
23. Borowicz S, Scoyk M, Avasarala S, Rathinam M, Tauler J, Bikkavilli R , et al. The soft agar colony formation assay. J Vis Exp, 2014; (92): p. e51998. DOI: 10.3791/51998.
24. Jonkman J, Cathcart J, Xu F, Bartolini M, Amon J, Stevens K, et al. An introduction to the wound healing assay using live-cell microscopy. Cell Adh Migr, 2014; 8(5): p. 440-51. DOI: 10.4161/cam.36224.
25. Khlefat S, Bardaweel S. Celecoxib inhibits cancer growth through cyclooxygenase 2 (COX2) independent pathways in HepG2 hepatocellular carcinoma. Jordan J. Pharm. Sci., 2021; 14(4).
26. Liberti J, Locasale M. The Warburg effect: how does it benefit cancer cells? Trends Biochem Sci, 2016; 41(3): p. 211-218. DOI: 10.1016/j.tibs.2015.12.001.
27. Scafoglio C, Hirayama B, Kepe V, Liu J, Ghezzi C, Satyamurthy N, et al. Functional expression of sodium-glucose transporters in cancer. Proc Natl Acad Sci U S A, 2015; 112(30): p. E4111-E4119. DOI: 10.1073/pnas.1511698112.
28. Villani L, Smith B, Marcinko K, Ford R, Broadfield L, Green A, et al. The diabetes medication Canagliflozin reduces cancer cell proliferation by inhibiting mitochondrial complex-I supported

respiration. Mol Metab, 2016; 5(10): p. 1048-1056. DOI: 10.1016/j.molmet.2016.08.014.
29. Xu D, Zhou Y, Xie X, He L, Ding J, Pang S, et al. Inhibitory effects of canagliflozin on pancreatic cancer are mediated via the downregulation of glucose transporter-1 and lactate dehydrogenase A. Int J Oncol, 2020; 57(5): p. 1223-1233. DOI: 10.3892/ijo.2020.5120.
30. Zhou J, Zhu J, Yu S, Ma H, Chen J, Ding X, et al. Sodium-glucose co-transporter-2 (SGLT-2) inhibition reduces glucose uptake to induce breast cancer cell growth arrest through AMPK/mTOR pathway. Biomed Pharmacother, 2020; 132: p. 110821. DOI: 10.1016/j.biopha.2020.110821.
31. Ota T, Xu L. Emerging roles of SGLT2 inhibitors in obesity and insulin resistance: Focus on fat browning and macrophage polarization. Adipocyte, 2018; 7(2): p. 121-128. DOI: 10.1080/21623945.2017.1413516.
32. Dasari S, Tchounwou P. Cisplatin in cancer therapy: molecular mechanisms of action. Eur J Pharmacol, 2014; 740: p. 364-78. DOI: 10.1016/j.ejphar.2014.07.025.
33. Joerger A, Fersht A. The p53 pathway: origins, inactivation in cancer, and emerging therapeutic approaches. Annu Rev Biochem, 2016; 85: p. 375-404. DOI: 10.1146/annurev-biochem-060815-014710.
34. Song Z, Zhu J, Wei Q, Dong G, Dong Z. Canagliflozin reduces cisplatin uptake and activates Akt to protect against cisplatin-induced nephrotoxicity. Am J Physiol Renal Physio, 2020; 318(4): p. F1041-F1052. DOI: 10.1152/ajprenal.00512.2019.
35. Thorn C, Oshiro C, Marsh S, Hernandez-Boussard T, McLeod H, Klein T, et al. Doxorubicin pathways: pharmacodynamics and adverse effects. Pharmacogenet Genomics, 2011; 21(7): p. 440-6. DOI: 10.1097/FPC.0b013e32833ffb56.
36. Zhong J, Sun P, Xu N, Liao M, Xu C, Ding Y, et al. Canagliflozin inhibits p-gp function and early autophagy and improves the sensitivity to the antitumor effect of doxorubicin. Biochem Pharmacol, 2020; 175: p. 113856. DOI: 10.1016/j.bcp.2020.113856.
37. Mirkin S, Pickar J. Selective estrogen receptor modulators (SERMs): a review of clinical data. Maturitas, 2015; 80(1): p. 52-57. DOI: 10.1016/j.maturitas.2014.10.010.
38. Aljanabi R, Alsous L, Sabbah D, Gul H, Gul M, Bardaweel S. Monoamine Oxidase (MAO) as a Potential Target for Anticancer Drug Design and Development. Molecules, 2021; 26(19): p. 6019. DOI: 10.3390/molecules26196019.
39. Boekhorst V, Preziosi L, Friedl P, Plasticity of cell migration in vivo and in silico. Annu Rev Cell Dev Biol, 2016; 32: p. 491-526. DOI: 10.1146/annurev-cellbio-111315-125201.
40. Pijuan J, Barcelo C, Moreno D, Maiques O, Siso P, Marti R, et al. In vitro cell migration, invasion, and adhesion assays: from cell imaging to data analysis. Front Cell Dev Biol, 2019; 7: p. 107. DOI: 10.3389/fcell.2019.00107.
41. Bhattacharya R, Fan F, Wang R, Ye X, Xia L, Boulbes D, et al. Intracrine VEGF signalling mediates colorectal cancer cell migration and invasion. Br J Cancer, 2017; 117(6): p. 848-855. DOI: 10.1038/bjc.2017.238.
42. Meng X, Jin Y, Yu Y, Bai J, Liu G, Zhu J, et al. Characterisation of fibronectin-mediated FAK signalling pathways in lung cancer cell migration and invasion. Br J Cancer, 2009; 101(2): p. 327-334. DOI: 10.1038/sj.bjc.6605154.
43. Verbeek B, Adriaansen-Slot S, Vroom T, Beckers T, Rijksen G. Overexpression of EGFR and c-erbB2 causes enhanced cell migration in human breast cancer cells and NIH3T3 fibroblasts. FEBS Lett, 1998; 425(1): p. 145-150. DOI: 10.1038/sj.bjc.6602184.
44. Borowicz S, Scoyk M, Avasarala S, Rathinam M, Tauler J, Bikkavilli R , et al. The soft agar colony formation assay. J Vis Exp, 2014; (92). DOI: 10.3791/51998.
45. Krysko D, Barghe T, D'Herde K, Vandenabeele P. Apoptosis and necrosis: detection, discrimination and phagocytosis. Methods, 2008; 44(3): p. 205-221. DOI: 10.1016/j.ymeth.2007.12.001.
46. Yamamoto L, Yamashita S, Nomiyama T, Hamaguchi Y, Shigeoka T, Horikawa T, et al. Sodium-glucose cotransporter 2 inhibitor canagliflozin attenuates lung cancer cell proliferation in vitro. Diabetol Int, 2021; p. 1-10. DOI: 10.1007/s13340-021-00494-6.
47. Wong M, Medrano J. Real-time PCR for mRNA quantitation. Biotechniques, 2005; 39(1): p. 75-85. DOI: 10.2144/05391rv01.
48. Pradeep C, Sunila E, Kuttan G. Expression of vascular endothelial growth factor (VEGF) and VEGF receptors in tumor angiogenesis and malignancies. Integr Cancer Ther, 2005; 4(4): p. 315-321. DOI: 10.1177/1534735405282557.
49. Tzifi F, Economopoulou C, Gourgiotis D, Ardavanis A, Papageorgiou S, Scorilas A. The role of BCL2 family of apoptosis regulator proteins in acute and chronic leukemias. Adv Hematol, 2012. 2012; DOI: 10.1155/2012/524308.

***

Supplement to Exploring the Role of Sodium-Glucose Cotransporter as a New Target for Cancer Therapy. J Pharm Pharm Sci (www.cspsCanada.org) 25, 253 - 265, 2022

Table 1S. Primers' forward and reverse sequences of each gene. SGLT2: gene for Sodium-glucose cotransporter 2; Bcl-2: gene for B-cell lymphoma 2; VEGF: gene for Vascular endothelial growth factor; GAPDH: gene for Glyceraldehyde 3-phosphate dehydrogenase.

Primer	Primer sequences
SGLT2	forward: 5-GATTTACACGGTGACAGGAGGG-3
	reverse: 5-CGGAGCAGGTGGTAGGAGT-3
Bcl-2	forward: 5-TTGTGGCCTTCTTTGAGTTCGGTG -3
	reverse: 5- GGTGCCGGTTCAGGTACTCAGTCA-3
VEGF	forward: 5-CTACCTCCACCATGCCAAGT-3
	reverse: 5-GCAGTAGCTGCGCTGATAGA-3
GAPDH	forward: 5-ACAACTTTGGTATCGTGGAAGG-3
	reverse: 5-GCCATCACGCCACAGTTTC-3

Table 2S. **The 50% inhibitory concentration (IC_{50}) and fold changes values of combined canagliflozin, ipragliflozin and chemotherapeutic agents in different cell lines for 48 h at 1:5 and 1:10**

A-549 cell line					
		1:5 ratio		**1:10 ratio**	
Cisplatin: Canagliflozin	IC_{50} in ratio	72.9	241	53.7	325.6
	Fold increase	1.6	3.4	1.2	4.6
Cisplatin: Ipragliflozin	IC_{50} in ratio	51.8	259.1	48.3	483.7
	Fold increase	1.1	1.2	1	2.3
Raloxifene: Canagliflozin	IC_{50} in ratio	18.5	55.4	6.4	64.3
	Fold reduction	2.2	1.2	6.3	1
Raloxifene: Ipragliflozin	IC_{50} in ratio	26.5	131.4	12.9	129.9
	Fold reduction	1.5	1.5	3.1	1.5
Caco-2 cell line					
		1:5 ratio		**1:10 ratio**	
Doxorubicin: Canagliflozin	IC_{50} in ratio	3	11.2	1.7	11.2
	Fold reduction	2.9	4.3	5.1	4.3
Doxorubicin: Ipragliflozin	IC_{50} in ratio	8.1	30.6	6.3	22.1
	Fold reduction	1.1	5.5	1.4	7.4
MCF-7 cell line					
		1:5 ratio		**1:10 ratio**	
Doxorubicin: Canagliflozin	IC_{50} in ratio	2.1	11.6	3.5	24
	Fold reduction	4.1	3.5	2.5	1.7
Doxorubicin: Ipragliflozin	IC_{50} in ratio	3.5	18.3	3.6	27.6
	Fold reduction	2.5	3.4	2.4	2.3
Raloxifene: Canagliflozin	IC_{50} in ratio	4.5	19.7	2.4	23.2
	Fold reduction	6.6	2.1	12.5	1.8
Raloxifene: Ipragliflozin	IC_{50} in ratio	13	57.3	5.4	35.4
	Fold reduction	2.3	1.1	5.6	1.7
Du-145 cell line					
		1:5 ratio		**1:10 ratio**	
Cisplatin: Canagliflozin	IC_{50} in ratio	12	58.4	6.7	65.5
	Fold increase	2	1.3	1.1	1.4
Cisplatin: Ipragliflozin	IC_{50} in ratio	35.5	175.6	18.8	185.9
	Fold increase	6.1	1.1	3.2	1.1
Pnac-1 cell line					
		1:5 ratio		**1:10 ratio**	
Cisplatin: Canagliflozin	IC_{50} in ratio	43.6	218.5	62.8	654.5
	Fold increase	1.3	4.7	1.8	14.2
Cisplatin: Ipragliflozin	IC_{50} in ratio	63.3	322.7	33.5	335.7
	Fold increase	1.8	1.2	1.0	1.3

Table 3S. Combination index (CI) values for combined treatment of SGLT2 inhibitors and other chemotherapeutic agents against different cell lines for 48h at different ratios.

A-549 cell line				
	Cisplatin: Canagliflozin		**Cisplatin: Ipragliflozin**	
Combination ratio	1:5	1:10	1:5	1:10
Combination index	1.9	1.8	1.5	1.3
	Raloxifene: Canagliflozin		**Raloxifene: Ipragliflozin**	
Combination ratio	1:5	1:10	1:5	1:10
Combination index	0.73	0.89	0.89	0.92
MCF-7 cell line				
	Raloxifene: Canagliflozin		**Raloxifene: Ipragliflozin**	
Combination ratio	1:5	1:10	1:5	1:10
Combination index	0.34	0.19	0.68	0.32
	Doxorubicin: Canagliflozin		**Doxorubicin: Ipragliflozin**	
Combination ratio	1:5	1:10	1:5	1:10
Combination index	0.35	0.74	0.87	0.44
Caco-2 cell line				
	Doxorubicin: Canagliflozin		**Doxorubicin: Ipragliflozin**	
Combination ratio	1:5	1:10	1:5	1:10
Combination index	0.44	0.82	0.59	0.27
Du-145 cell line				
	Cisplatin: Canagliflozin		**Cisplatin: Ipragliflozin**	
Combination ratio	1:5	1:10	1:5	1:10
Combination index	1.9	2.8	1.5	4.5
Panc-1 cell line				
	Cisplatin: Canagliflozin		**Cisplatin: Ipragliflozin**	
Combination ratio	1:5	1:10	1:5	1:10
Combination index	2.5	1.4	2	3.2